ACS APPLIED MATERIALS & INTERFACES

Research Article

www.acsami.org

Spectroscopic Study of the Photofixation of SO_2 on Anatase TiO_2 Thin Films and Their Oleophobic Properties

Z. Topalian,*[,†] G. A. Niklasson,[†] C. G. Granqvist,[†] and L. Österlund[†,‡]

[†]Department of Engineering Sciences, The Ångström Laboratory, Uppsala University, P.O. Box 534, SE-751 21 Uppsala, Sweden

[‡]FOI, Cementvägen 20, SE-901 82 Umeå, Sweden

ABSTRACT: Photoinduced SO_2 fixation on anatase TiO_2 films was studied by in situ Fourier transform infrared (FTIR) and X-ray photoelectron spectroscopy (XPS). The TiO_2 films were prepared by reactive DC magnetron sputtering and were subsequently exposed to 50 ppm SO_2 gas mixed in synthetic air and irradiated with UV light at substrate temperatures between 298 and 673 K. Simultaneous UV irradiation and SO_2 exposure between 373 and 523 K resulted in significant sulfur (S) deposits on crystalline TiO_2 films as determined by XPS, whereas amorphous films contained negligible amounts of S. At substrate temperatures above 523 K, the S deposits readily desorbed from TiO_2. The oxidation state of sulfur successively changed from S^{4+} for SO_2 adsorbed on crystalline TiO_2 films at room temperature without irradiation to S^{6+} for films exposed to SO_2 at elevated temperatures with simultaneous irradiation. In situ FTIR was used to monitor the temporal evolution of the photoinduced surface reaction products formed on the TiO_2 surfaces. It is shown that band gap excitation of TiO_2 results in photoinduced oxidation of SO_2, which at elevated temperatures become coordinated to the TiO_2 lattice through interactions with O vacancies and form sulfite and sulfate surface species. These species makes the surface acidic, which is manifested in nondetectable adherence of stearic acid to the modified surface. The modified films show good chemical stability as evidenced by sonication and repeated recycling of the films. The results suggest a new method to functionalize wide band gap oxide surfaces by means of photoinduced reactions in reactive gases at elevated substrate temperatures. In the case of anatase TiO_2 in reactive SO_2 gas, we here show that such functionalization yields surfaces with excellent oleophobic properties, as probed by adhesion of stearic acid.

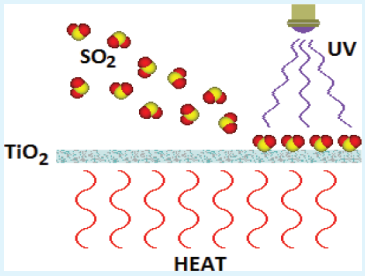

KEYWORDS: *TiO_2, SO_2, photofixation, FTIR, XPS*

Titanium dioxide (TiO_2) is a semiconducting oxide which has been thoroughly studied for a variety of applications such as biomaterials, pigments, electronics, sensors, and catalysts,[1−3] all of which derive from the fundamental materials properties of TiO_2. The most common TiO_2 modifications, anatase and rutile, comprise 6-fold coordinated Ti atoms in an octahedral configuration. The Ti−O bonding has pronounced ionic character, which makes TiO_2 thermodynamically stable under atmospheric conditions in a wide temperature range (with the rutile phase being the most stable). TiO_2 has an electronic structure which exhibits a wide band gap (about 3.2 and 3.0 eV for anatase and rutile, respectively) with the conduction band straddling the affinity level for molecular oxygen. It is thus optically transparent, and small TiO_2 particles appear white. The TiO_2 surface has amphoteric surface chemical properties which are amenable to selective acidic/basic reactions. The latter has, e.g., been exploited in the Claus reaction,[4] i.e., the catalytic recovery of sulfur from acidic gases containing hydrogen sulfide. In a modified reaction scheme, this reaction includes partial oxidation of H_2S to SO_2 in a first step prior to further oxidation to water and sulfur. While traditional γ-Al_2O_3 catalysts show pronounced deactivation due to sulfur deposits, TiO_2 both promotes H_2S and SO_2 oxidation and at the same time avoids irreversible sulfur deactivation. This is due to a Mars-Van Krevelen type reaction between lattice oxygen in TiO_2 and adsorbed sulfur which replenishes the catalyst in an oxidizing atmosphere.[5]

Gas sensing with semiconducting metal oxide thin films has been the subject of several studies during the last decades, and these films are promising candidates for versatile and inexpensive gas sensors.[6] TiO_2 has been studied as a gas sensor material, and the effect of ultraviolet (UV) irradiation on the resistance response has been investigated.[7,8] Detection of malodorous and toxic compounds such as H_2S and SO_2 are highly desirable but at the same time challenging with oxide sensors. These molecules represent two possible types of interactions which are expected to modify the electron transport properties differently: SO_2 is an electron acceptor while H_2S is an electron donor molecule. Indeed, interactions of these molecules with TiO_2 were reported to decrease and increase the conductivity, respectively.[5] The sensitivity of any oxide sensor is however challenging. The odor threshold for H_2S is very low (0.5 ppb) and several decades lower than SO_2 (0.5 ppm); the corresponding threshold limit values are 10 and 2 ppm, respectively.[9] Furthermore, reactions of the gas molecules with TiO_2 may cause sensor deactivation by means of sulfur

Received: September 16, 2011
Accepted: December 28, 2011
Published: December 28, 2011

compound deposits (in particular at low operation temperatures). TiO_2 is also a well-known photocatalytic material, which has been the subject of intense research during the last decades.[2,10] Thus, apart from modulated conduction, photoinduced surface reactions may also be anticipated. The latter may introduce difficulties with regard to the interpretation of the sensor response, but it can also yield additional information that may be used to separate signal responses and thus increase sensor selectivity.

In this paper, we report on the molecular interaction of SO_2 with TiO_2 with and without UV irradiation at various substrate temperatures from room temperature up to 673 K. The latter value is important because it is in the temperature range where most oxide sensors based on conduction/resistivity measurements operate. Our results show that SO_2 is photofixated to TiO_2 at elevated temperatures with a resulting acidification of the TiO_2 surface. Indeed, we find, quite unexpectedly, that the surface chemical properties of the films can be purposefully modified by SO_2 photofixation to fabricate films exhibiting oleophobic properties. In addition, our results provide insights into molecular reaction mechanisms pertinent to, e.g., desulfurization catalysis. By use of in situ Fourier transform infrared (FTIR) spectroscopy and X-ray photoelectron spectroscopy (XPS), we show that UV irradiation of nanostructured TiO_2 films in synthetic air at elevated temperature stimulates SO_2 photofixation, and we propose a mechanism that accounts for these findings.

2. EXPERIMENTAL SECTION

2.1. Film Deposition. Titanium dioxide films were prepared by reactive DC magnetron sputtering in a deposition system based on a Balzers UTT 400 unit as described before.[7] The sputtering chamber was evacuated to $\sim 10^{-7}$ Torr by turbo molecular pumping and was baked for 8 h at ~373 K to achieve a low base pressure and to remove contaminants from the sputter chamber. Argon (99.998%) and oxygen (99.998%) were introduced via separate mass-flow controlled inlets so that the O_2/Ar gas flow ratio was maintained at 0.067. Two magnetron sources, arranged in an oblique angle setup, were used for sputtering Ti from 99.99% pure metallic targets. The targets were 51 mm in diameter and 5.6 mm thick. The sputter plasma was generated at a constant current of 750 mA and at a total pressure of ~40 mTorr. During the film deposition process, the substrates were rotated with a speed of ~50 rpm in order to avoid formation of preferentially oriented structures. Prior to the deposition, the Ti targets were presputtered in argon for 10 min in order to remove oxides and other possible contaminants. Deposition of ~1 μm thick TiO_2 films was made on CaF_2 and Si(100) substrates at room temperature. The film thickness was determined by surface profilometry over a step edge using a Tencor Alpha-Step instrument. Some of the films were annealed in air at 773 K for 1 h in an oven with a temperature stabilization of ±2 K. Detailed information about TiO_2 film preparation and characterization can be found elsewhere.[7,11]

2.2. Materials Characterization. Grazing incidence X-ray diffraction showed that as-deposited TiO_2 films exhibited an amorphous structure with only small traces of crystallinity; they are here denoted a-TiO_2. In contrast, the annealed films were highly crystalline with distinct diffraction peaks corresponding to pure anatase and are denoted c-TiO_2.

X-ray photoelectron spectroscopy (XPS) was performed on a PHI Quantum 2000 ESCA system with a monochromatic Al Kα radiation source and a low-energy electron flood gun for charge compensation. High-resolution scans were obtained using pass energy of 23.5 eV and an energy resolution of 0.1 eV. The binding energy (BE) scale was calibrated against the aliphatic C1s peak at 284.8 eV from adventitious carbon on the surface. The Shirley background routine was used for background corrections of the XPS spectra.

2.3. In Situ FTIR Spectroscopy. Fourier transform infrared (FTIR) spectroscopy measurements were performed between 800 and 4000 cm^{-1} using a vacuum spectrometer (Bruker IFS66v/S) equipped with a liquid nitrogen cooled narrow-band HgCdTe detector as described earlier.[12] All FTIR measurements were carried out in a custom-modified transmission reaction gas cell allowing for in situ reaction studies at controlled sample temperature with simultaneous FTIR spectroscopy, gas dosing, and light irradiation in a controlled atmosphere. Irradiation was done with a UV light emitting diode (LED), which emitted light at 370 nm with a full width at half-maximum of 12 nm. The output from the LED was 1 mW cm^{-2} at the sample position (at a distance of ~1 cm from the source) as measured with a calibrated thermopile detector (Ophir). Repeated FTIR spectra were recorded as a function of irradiation time every 30 s with 4 cm^{-1} resolution; each spectrum was averaged over 69 scans. Absorbance A was determined from measured transmission (τ) after appropriate baseline corrections of the spectral data from the relation $A = -\log(\tau)$.

FTIR spectra were acquired with the samples kept at a substrate temperature, T_s = 373, 423, and 473 K, respectively, and a 100 mL min^{-1} gas flow of synthetic air through the reaction cell. Prior to each measurement, the samples were cleaned at 673 K in 100 mL min^{-1} synthetic air for 15 min and were subsequently cooled to the desired temperature before data acquisition. In all measurements, the FTIR background was collected on a clean sample in a synthetic air feed and at the working temperature. SO_2 gas at 50 ppm was added to the gas, and the sample was irradiated with UV light. Repeated IR spectra were recorded as a function of reaction time with intermittent dark and UV irradiation periods (10 min dark and 10 min light). The TiO_2 films used for FTIR measurements where deposited on CaF_2 substrates.

2.4. Gas Exposure. Systematic SO_2 exposures of several as-deposited and annealed films of TiO_2 were performed in a dedicated reaction cell.[11] The reaction gas was admitted into the reaction cell through a set of mass-flow controllers. A gas flow of 50 ppm SO_2 in synthetic air with a total gas feed of 200 mL min^{-1} was employed. Gas exposure was made for 1 h under UV irradiation using a source consisting of a cluster of 24 LEDs of the same type as those employed in the in situ FTIR experiments described above. The distance between the UV source and the sample was 10 cm, which ensured an even distribution of the light intensity on the sample. The gas exposure was conducted at sample temperatures between 293 and 673 K. Elevated temperatures were obtained by the use of a copper-based heating plate comprising a heating cartridge and a thermocouple regulated by a Hanyoung PX9 digital temperature controller.

2.5. Sonication. In order to check the chemical stability of the SO_2 modified films, the films were sonicated in deionized water for 15 min in an ultrasonic bath (Sonorex Super RK100H) using high-frequency power (80 W and 35 kHz). The sonicated films were prepared on silicon substrates; this was necessary since films on CaF_2 readily peeled off during sonication.

2.6. Stearic Acid Spin-Coating. The oleophobic properties of pure and SO_2-modified TiO_2 films prepared at T_s = 473 K were characterized by examining the adherence of stearic acid as previously described.[11] Briefly, stearic acid was applied to the sample surfaces by deposition of 10 mm^3 of a 0.8 mM methanol solution and spin coating at 1500 rpm. The concentration of stearic acid on the films was measured using transmission FTIR spectroscopy. Repeated spin coating of stearic acid was made after rinsing the samples between each experiments. Samples were cleaned by rinsing in isopropanol, acetone, and deionized water and subsequently heat-treated in an oven at 80 °C for 5 min in order to remove solvents. The samples were then placed in the IR spectrometer and kept there for 15 min before background measurement. In all measurements, the FTIR background was collected on a clean sample in open air. Stearic acid was then spin coated on the samples, and the IR absorbance was measured. Three cycles of measurements were performed on the SO_2-modified TiO_2 samples in order to examine the durability of their surface acid properties. The TiO_2-based samples used in these experiments were deposited on CaF_2 substrates, and the SO_2-modified TiO_2 sample was the same one that was used in in situ FTIR experiments carried out at T_s = 473 K described above.

3. RESULTS AND DISCUSSION

3.1. XPS. Figure 1 shows high-resolution XPS spectra of the S2p region obtained on crystalline TiO_2 films deposited on

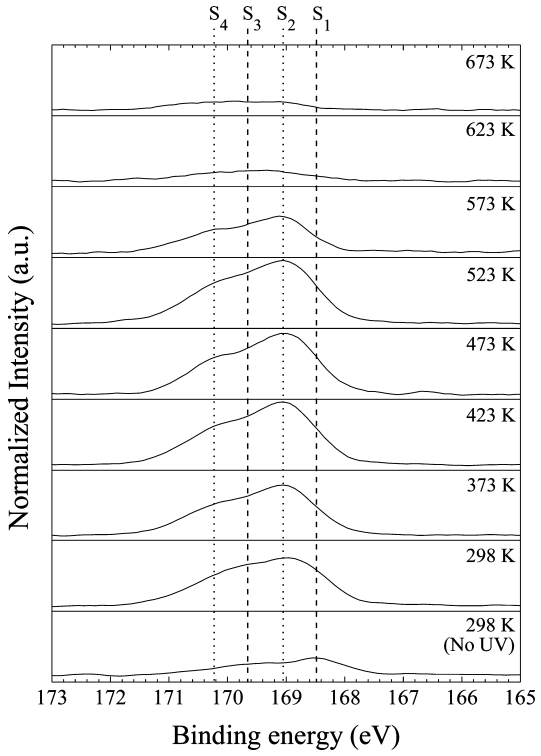

Figure 1. XPS S2p spectra of TiO_2 films treated at different T_s in 50 ppm SO_2 gas with and without UV irradiation. The $S2p_{1/2}$ and $S2p_{3/2}$ peaks in S^{4+} are labeled S_3 and S_1, respectively, and the $S2p_{1/2}$ and $S2p_{3/2}$ peaks in S^{6+} are labeled S_4 and S_2, respectively.

CaF_2 substrates and exposed to SO_2 gas under different conditions in the reaction cell. The peaks labeled S_1, S_2, S_3, and S_4 can be identified with the $S2p_{1/2}$ and $S2p_{3/2}$ peaks in S^{4+} and S^{6+}, respectively.[13] Thus, the peaks labeled S_3 and S_1 correspond to the $S2p_{1/2}$ and $S2p_{3/2}$ states in S^{4+}, respectively, and the peaks labeled S_4 and S_2 correspond to $S2p_{1/2}$ and $S2p_{3/2}$ states in S^{6+}, respectively. The measured binding energy (BE) peak separations (S_4–S_2) and (S_3–S_1) are 1.18 ± 0.01 and 1.17 ± 0.02 eV, respectively (Table 1). This is in excellent agreement with handbook data (1.18 eV).[13] The relative intensities of S_1 to S_3 and S_2 to S_4 peaks is determined to be about 2:1, which agrees with the expected result considering the degeneracy of the spin–orbit splitting. After UV irradiation at T_s < 423 K, an intermediate S^{5+} oxidation state may be discerned in Figure 1, but an overlapping contribution from several simultaneously occurring states prevents an unambiguous determination of the corresponding BE. Analysis of the S2p peak binding energies and relative peak intensities and comparisons with reported data for different chemical states of S show that at T_s = 298 K and without UV irradiation mainly S^{4+} species are present on the c-TiO_2 films.

UV irradiation at T_s = 298 K results in an increasing concentration of species with higher oxidation states (S^{5+} and S^{6+}). From Figure 2, it is evident that the relative concentration of

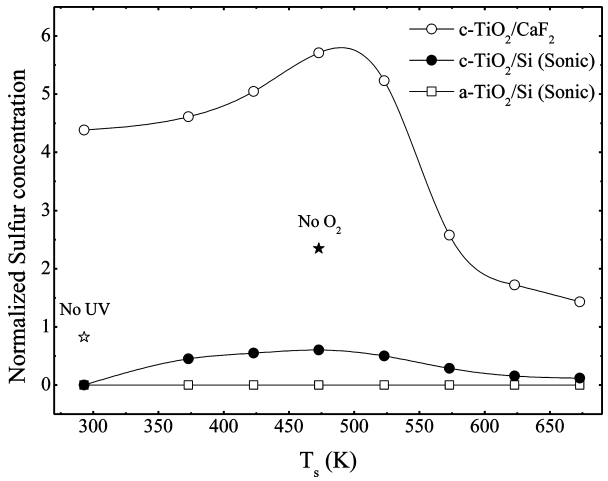

Figure 2. Normalized sulfur concentration (atom % S2p/Ti2p × 100) in crystalline (circles) and amorphous (squares) TiO_2 films as a function of T_s. The hollow and solid stars denote the S concentration in c-TiO_2 films exposed to 50 ppm SO_2 without UV irradiation and in absence of O_2, respectively. The curves were drawn for convenience. Note that sonication experiments were performed on films backed by Si substrates.

S^{6+} to S^{4+} increases with increasing T_s. At $T_s \geq$ 373 K, films contain mainly S^{6+} species thus proving that the photofixated SO_2 species are oxidized and are associated with sulfate surface species. At the highest T_s, only small amounts of S^{6+} species remain on the surface, which shows that most S species desorb above 600 K in agreement with results in previous studies.[5] Figure 2 summarizes the measured S concentration in the same TiO_2 films as those reported in Figure 1. The concentrations were calculated as the ratio of the atomic concentration of S and Ti determined from XPS survey scans, which facilitates intersample comparisons. For comparison, the corresponding compositions (in atom %) determined from XPS survey scans are shown in Table 1. It is seen that the S concentration in c-TiO_2 films increases up to $T_s \approx$ 500 K when they are exposed to 50 ppm SO_2 gas in synthetic air and are simultaneously UV irradiated. Above 500 K, the S concentration decreases

Table 1. Elemental Composition (atom %) from XPS Survey Scans and Binding Energy (BE) of c-TiO_2 Films Exposed to 50 ppm SO_2 Gas under UV Irradiation at Different Temperatures

	273 K (no UV)		273 K		473 K		523 K		573 K		673 K	
	BE	atom %	BE	atom %	BE	atom %	BE	atom %	BE	atom %	BE	atom %
O1s	529.49	55.91	529.88	57.15	530.08	56.16	530	58.49	530.03	57.99	530	65.3
C1s	284.6	14.75	284.6	14.26	284.6	14.41	284.6	13.56	284.6	13.37	284.6	7.06
$Ti2p_{3/2}$	458.6	29.1	458.65	27.39	458.8	27.84	458.75	26.57	458.78	27.93	458.7	27.3
$Ti2p_{1/2}$	464.14		464.19		464.34		464.29		464.32		464.24	
$S2p_{3/2}$	168.48	0.24	168.97	1.2	169.05	1.59	169.05	1.39	169.12	0.72	169.33	0.39
$S2p_{1/2}$	169.66		170.15		170.23		170.23		170.3		170.51	

dx.doi.org/10.1021/am201253y | ACS Appl. Mater. Interfaces 2012, 4, 672–679

abruptly. On the other hand, the S concentration in amorphous TiO_2 films is much smaller regardless of T_s and UV irradiation (data not shown). In the absence of UV irradiation, the S concentration is much lower in c-TiO_2 films. Similarly, the S concentration in c-TiO_2 films is much lower in the absence of O_2 in the feed gas. These results indicate that SO_2 reacts photochemically with TiO_2 and that both O_2 and elevated T_s promote photofixation of SO_2. The effect of O_2 suggests that band gap irradiation of TiO_2 produces conduction electrons that react with adsorbed oxygen to form oxygen radicals which further react with SO_2, and the effect of T_s indicates that O vacancies are formed at elevated temperature and provide adsorption sites for photoreacted SO_2.

Figure 2 also shows corresponding XPS results obtained after 15 min of vigorous sonication of TiO_2 films deposited on Si(100) wafers and prepared in SO_2 gas at different T_s. Figure 2 demonstrates that S is completely removed from a-TiO_2 films after sonication, while significant amounts remain in the c-TiO_2 films treated at T_s of 373 to 523 K. This indicates that SO_2 reacts with TiO_2 and forms chemically strong bonds with the c-TiO_2 films irradiated at elevated T_s. Furthermore, comparing the S concentration and BE for nonsonicated and sonicated films at different T_s, we conclude that S exists in different chemical forms at 293 K and at elevated T_s. At low T_s, most S is removed by sonication which suggests that it is associated with weakly bonded S species such as $SO_{2,ad}$ and H_2SO_4, while at higher T_s a significant fraction of S is associated with strongly bonded sulfate species. This is further proved by the in situ FTIR data discussed below.

3.2. In Situ FTIR. With in situ FTIR, it is possible to follow the photoinduced surface reactions as a function of time which precede the sulfur fixation on the TiO_2 films seen in XPS and to identify the strongly bonded SO_2-derived surface species that forms on TiO_2. We first present results obtained after SO_2 exposure and UV irradiation. Figure 3 depicts FTIR spectra

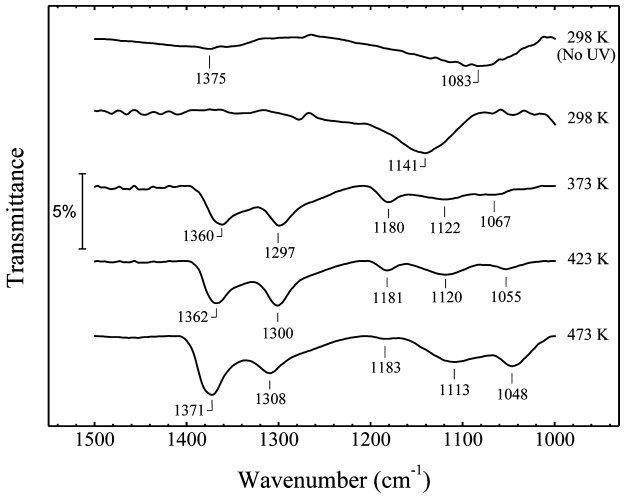

Figure 3. In situ FTIR transmission spectra obtained in synthetic air during UV irradiation of c-TiO_2 films treated at different T_s from 298 to 473 K after 30 min of UV irradiation in 50 ppm SO_2 gas. The top spectrum shows spectra obtained at 298 K after 10 min SO_2 exposure without UV irradiation.

obtained after exposure to 50 ppm SO_2 in synthetic air at different T_s with and without simultaneous UV irradiation. The spectrum obtained without UV absorption exhibits weak absorption bands, which may be attributed to adsorbed SO_2 and SO_2^- ions (Figure 3, top spectrum).[14−16] This result is also consistent with the existence of predominantly S^{4+} (and S^{5+}) species in XPS. After UV irradiation, SO_2 becomes oxidized and is successively converted to S^{6+} species with increasing T_s according to XPS. The FTIR spectrum shown in Figure 3 obtained after UV irradiation at 298 K exhibits a broad band centered at ∼1140 cm^{-1}. This band occurs at the same frequency as a previously reported band attributed to HSO_3^- due to interactions between SO_2 and water, or more specifically with basic OH^- groups on anatase,[17] and it may thus be associated with UV-induced reactions between SO_2 and surface OH^- groups.

At T_s > 373 K, most SO_2 is converted to S^{6+} species according to XPS. In the FTIR spectra, new absorption bands develop at ∼1360, ∼1300, ∼1180, ∼1120, and ∼1055 cm^{-1} for $T_s \geq 373$ K. The low-wavenumber bands are typical for sulfite and sulfate groups that coordinate to basic O^{2-} and Ti Lewis sites, respectively.[14,18,19] In particular, the 1180 cm^{-1} band indicates the presence of adsorbed SO_3^- species (supporting the assertion from XPS that there is a mix of several oxidation states of S, which gradually transform into S^{6+} at the highest T_s).[15] The pronounced band at ∼1300 cm^{-1}, whose intensity increases up to 473 K, can be attributed to SO_2 adsorbed to low-coordinated Ti in O vacancy sites which can be described as Ti−SO_2^- ions.[20] This is in good agreement with previous observations[5] and consistent with the temperature dependence of surface O vacancy formation.[1,21] Alternatively, SO_2 species bonded to Ti^{3+} interstitials that diffuse to the surface region may be considered.[22] Absorption bands between 1300 and 1400 cm^{-1} are typically observed for coordinated SO_2 species (the asymmetric ν_{as}(O═S═O) modes), but such an association would contradict the XPS data which unambiguously shows that the concentration of S^{6+} species increases at elevated temperatures, while the concentration of S^{4+} species decreases at high T_s. Moreover, the sonication experiments show that the species connected with the absorption bands between 1300 and 1400 cm^{-1} are strongly bonded to the TiO_2 surface. Thus, we infer that these species must be due mainly to surface coordinated S^{6+} species. The experimental circumstances described above suggest that these species are photooxidized SO_2 bonded to O vacancy sites such as coordinated Ti−SO_4^{2-} species or more generally Ti−$SO_4^{\delta-}$ species, depending on the bond order and oxidation state of the surface Ti atoms. This may also explain the different spectral profile in the 1200 to 1000 cm^{-1} region, compared to previously reported data, for adsorbed SO_2 discussed above. It should be noted that FTIR spectra shown in Figure 3 remain the same after subsequent periods of UV irradiation in absence of SO_2 in the feed gas, which shows that the photofixated SO_x species do not undergo further photoreactions in synthetic air.

Figure 4 shows the temporal evolution of the FTIR absorption bands acquired in SO_2 gas at T_s = 373 K. It is evident that before UV irradiation FTIR spectra resemble those acquired without irradiation at 298 K. In particular, the bands that initially develop at ∼1030, ∼1060, ∼1080, and ∼1140 cm^{-1} can be ascribed to a mixture of adsorbed SO_3^{2-},[14] SO_4^{2-},[18,19] SO_2^-,[15] and HSO_3^- species, respectively.[17] The ∼1140 cm^{-1} band attributed to HSO_3^- disappears after a few minutes along with the absorption bands due to isolated (basic) OH groups at 3685 and 3673 cm^{-1}, as seen in Figure 5.[23,24] No further depletion is observed upon repeated SO_2 exposure and UV irradiation, which supports the proposition by Shor et al.[17] that the ∼1140 cm^{-1} band is due to HSO_3^- formed by reaction

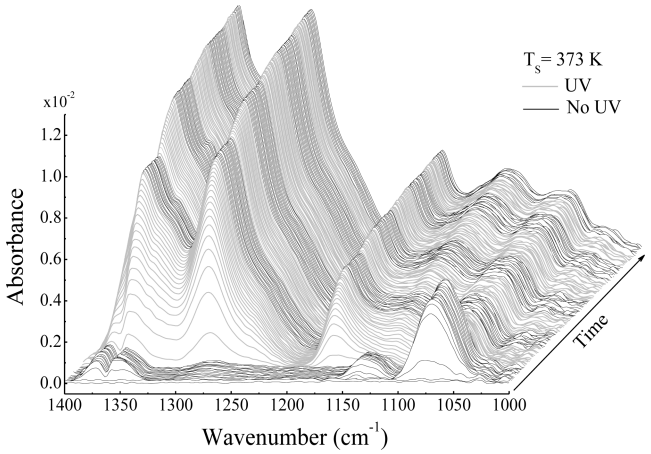

Figure 4. FTIR absorbance spectra acquired sequentially (bottom to top) during intermittent 10 min periods with and without UV irradiation in 50 ppm SO_2 and at T_s = 373 K during ~90 min. The gray (black) curves indicate periods with (without) UV irradiation. The first two bottom spectra were acquired in synthetic air prior to SO_2 gas admission to the reaction cell.

between SO_2 and basic OH^- surface groups and that these OH groups are consumed during the first few minutes of reactions at 373 K. However, as soon as UV irradiation commences, new absorption bands appear and grow rapidly as a function of irradiation time. Notably, bands between 1200 and 1400 cm^{-1}, attributed to coordinated sulfite and sulfate species as discussed above, appear and dominate the spectra after more than 5 min of UV irradiation. After the first 10 min UV irradi-ation period, these bands are almost saturated, which suggests that the accessible sites are saturated. It is also seen that these bands do not grow during periods with no UV irradiation, which proves that these absorption bands solely are due to photoinduced surface reactions. Figure 6 details the temporal evolution of the FTIR absorption bands at different T_s and at different times during intermittent dark periods and UV irradiation. The spectra at T_s = 373 K are the same as in Figure 4. By comparisons of the spectra prior to irradiation, it is seen that the concentration of HSO_3^- species (associated with the 1134 cm^{-1} band) becomes smaller with increasing T_s. At all T_s, a broad absorption band develops at ~1072 cm^{-1} during the first 10 min of SO_2 exposure in the dark. Again, this occurs simultaneously as isolated surface OH groups at 3685 and 3673 cm^{-1} disappear and shows that HSO_3^- is rapidly oxidized to sulfate ions. At all T_s between 373 and 473 K, new strong transmission bands develop in the 1370−1300 cm^{-1} region and at ~1180 and 1120−1110 cm^{-1} during the first UV exposure cycle at the same time as the broad band at 1071−1075 cm^{-1} decreases and vanishes. We note that during subsequent dark periods in SO_2 gas no new transmission bands develop at 1071−1075 cm^{-1} as during the first SO_2 adsorption period on the fresh TiO_2 surface. This is because all reactive surface OH groups have been consumed during the first irradiation period. Again, this is proved by following the simultaneous evolution of the OH bands in FTIR, as seen in Figure 5. Subsequent periods do not alter the OH spectral region. The surface OH groups which are consumed during the first adsorption cycle in the dark are not replenished. Figure 6 shows that the 1200−1400 cm^{-1} spectral region contains several peaks whose amplitude varies with T_s. In particular, the intensity of the ~1370 cm^{-1} peak increases relative to the ~1360 cm^{-1} peak as T_s increases. The 1180 cm^{-1}

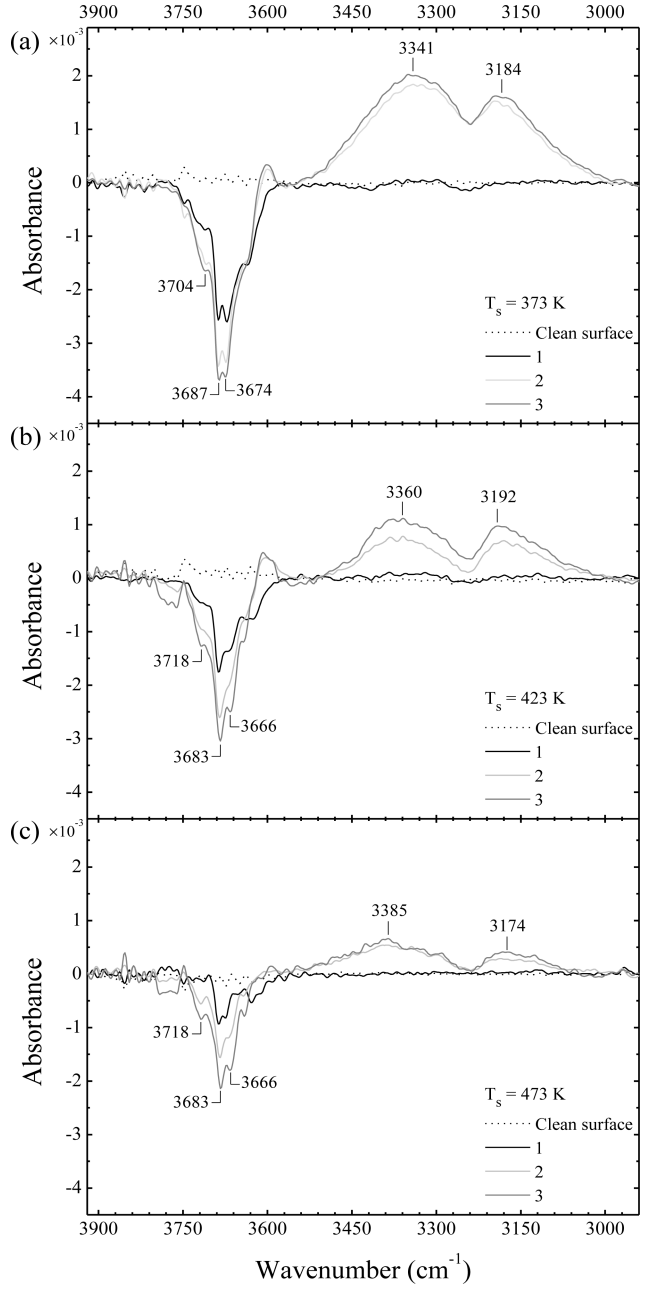

Figure 5. In situ FTIR spectra obtained after exposure of c-TiO_2 films to 50 ppm SO_2 in synthetic air for 10 min (spectrum 1) and after subsequent UV irradiation for 10 and 30 min in dark state (spectra 2 and 3), respectively, in the same feed gas at the shown values of T_s. The dotted curves indicate spectra obtained on clean c-TiO_2 in synthetic air prior to SO_2 exposure.

peak decreases as T_s increases, while the intensity and vibrational energy of the bands at ~1120 and ~1050 cm^{-1} increase and shift down. According to the discussion above, this suggests that SO_3^- is oxidized to SO_4^{2-} species at the highest T_s. Accordingly, we attribute the spectral modifications in the 1200−1400 cm^{-1} region to the corresponding redistribution of coordinated sulfite to sulfate surface species. We stress however that these assignments are tentative and that, to the best of our knowledge, no previous study on photofixation of SO_2 at elevated temperatures has been reported. Finally, it is evident that the integrated absorbance of the bands in the 1300−1370 cm^{-1} region increase from T_s = 373 K to T_s = 473 K. This shows that

dx.doi.org/10.1021/am201253y | ACS Appl. Mater. Interfaces 2012, 4, 672−679

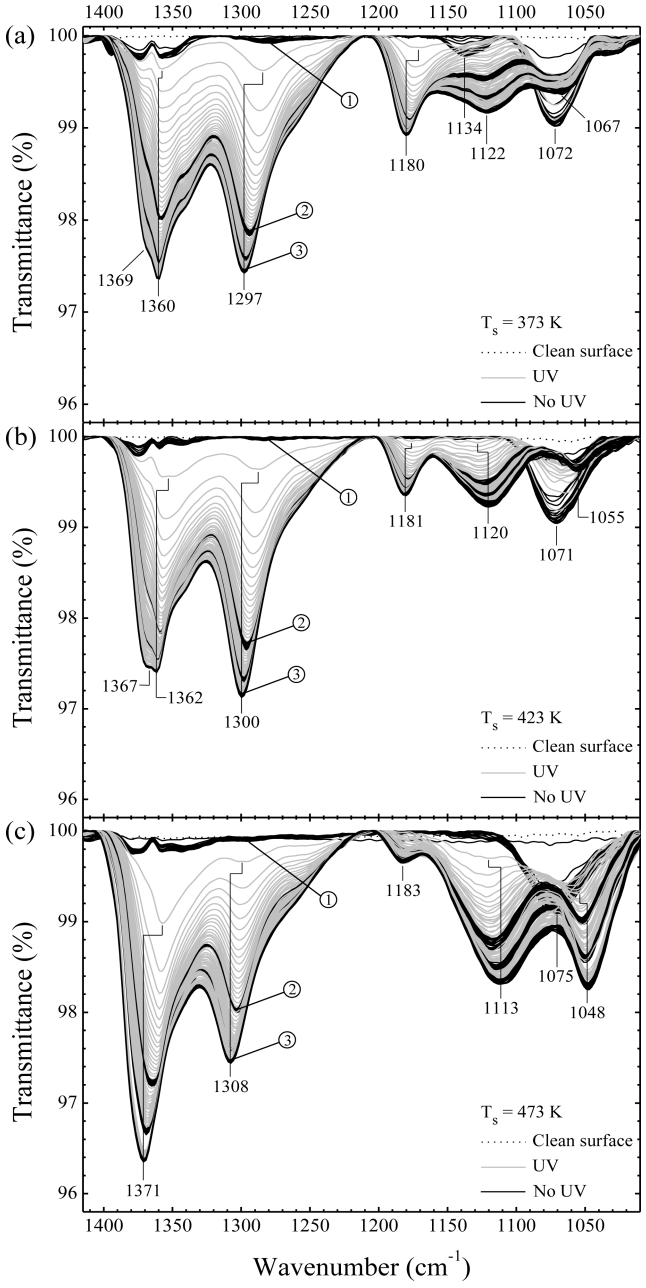

Figure 6. In situ FTIR spectra obtained during UV irradiation of c-TiO_2 films at the shown values of T_s and in 50 ppm SO_2 gas. Gray and black curves show the spectral evolution of transmission bands under intermittent 10 min of UV irradiation and dark periods. The dotted curves indicate spectra obtained on clean c-TiO_2 in synthetic air prior to SO_2 exposure. Spectra 1−3 correspond to the same irradiation times as spectra 1−3 in Figure 5.

the amount of photofixated SO_2 species increases up to 473 K in accordance with the XPS data.

The results above strongly support a reaction mechanism where adsorbed SO_2 reacts with O_2^- (or O^-) formed by band gap irradiation of TiO_2 to form sulfite and sulfate species. At elevated temperatures, the surface concentration of oxygen vacancies (and/or Ti^{3+}) increases, which provides sites for the oxidized SO_2 species. The combined XPS and FTIR results strongly suggest that the end-products of these reactions are surface coordinated sulfate species. The temperature dependence of the surface S concentration from XPS suggests that sulfate ions bind at O vacancy sites formed at elevated temperatures, since SO_2 molecules which bind with the S atom in the O vacancy site can be described as sulfate species. In contrast, SO_2 which bind to basic O^{2-} sites form surface coordinated sulfite.[14] The combined FTIR and XPS results show that SO_2 gradually transforms to sulfate species, which are thermodynamically stable up to ca. 500 K. In comparison with the modified Claus reaction, our suggested reaction can proceed at lower temperatures due to the photochemical formation of reactive oxygen species. The major reaction paths responsible for surface sulfate formation can be summarized as follows:

$$O_2 + 2e^- \xrightarrow{h\nu,TiO_2} {O_2}^{2-} \quad (1)$$

$$SO_{2,ad} + {O_2}^{2-} \rightarrow {SO_{4,ad}}^{2-} \quad (2)$$

An initial reaction pathway that involves basic surface OH groups has also been identified, viz.,

$$SO_{2,ad} + OH^- \xrightarrow{h\nu,TiO_2} HSO_{3,ad}{}^- \quad (3)$$

At elevated substrate temperatures, O vacancies, denoted V_O, provide reaction sites for the sulfate ions produced in reaction 2 and react with TiO_2 to form coordinated surface complexes, viz.,

$${SO_{4,ad}}^{2-} + V_O \xrightarrow{TiO_2} Ti{-}SO_4{}^{2-} \quad (4)$$

Moreover, it is evident from Figures 5 and 6 that there is a correlation between the amounts of photofixated SO_2 and consumed surface OH groups. This suggests that new SO_2 adsorption sites are created during UV irradiation. In analogy with the temperature activated formation of O vacancy sites in reaction 4 above, we propose that O vacancies also are formed via a photoreaction pathway:[25]

$$HO_{br} + H_{ad} \xrightarrow{h\nu,TiO_2} V_O + H_2O \quad (5)$$

with concomitant formation of H_2O as evident from Figure 5 (~ 3180−3340 cm^{-1} bands). This is a reverse analogue of the O vacancy promoted H_2O dissociation channel, which has been extensively for the rutile (110) surface;[25] SO_2 then reacts with these V_O sites,

$$SO_{2,ad} + V_O \xrightarrow{TiO_2} Ti{-}SO_{2,ad} \quad (6)$$

which then is further oxidized to sulfate according to reaction 2 above.

The integrated absorbance in the 1200−1400 cm^{-1} region was determined in order to quantify the amount of photofixated $SO_x^{\delta-}$ species on the c-TiO_2 films and to determine the formation kinetics at different T_s. The result is shown in Figure 7, which clearly shows that these species only form during UV irradiation and that the concentration, c, increases up to 473 K. Figure 8a shows the integrated FTIR absorbance, A, between 1205 and 1409 cm^{-1} associated with coordinated sulfite and sulfate species as a function of irradiation time. In Figure 8a, the data are normalized to the absorbance after 10 min irradiation, A_s, at each T_s. The formation kinetics is well described by first-order reaction kinetics, i.e., $c/c_s = 1 - \exp(-k_r t)$, where c_s is the saturation coverage (corresponding to A_s) and k_r is the formation rate constant (Figure 8a). It is seen that the rate of formation of the surface species increases with increasing T_s and suggests a thermally activated photofixation process. It is

dx.doi.org/10.1021/am201253y | ACS Appl. Mater. Interfaces 2012, 4, 672−679

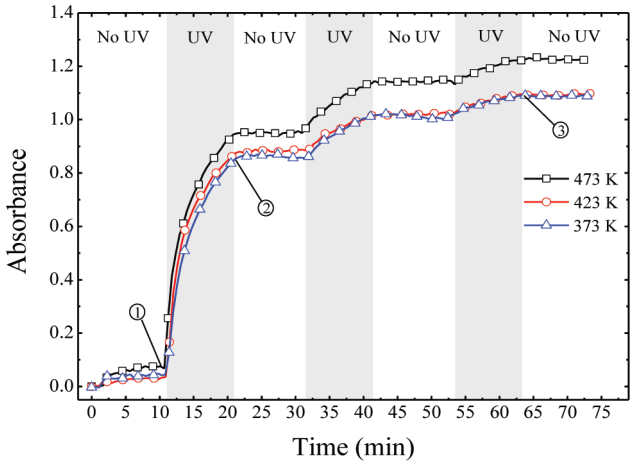

Figure 7. Integrated FTIR absorbance calculated between 1205 and 1409 cm^{-1} as a function of SO_2 exposure time at different T_s with and without simultaneous UV irradiation. The data correspond to the experiments reported in Figure 6. No. 1−3 corresponds to spectra 1−3 in Figures 5 and 6.

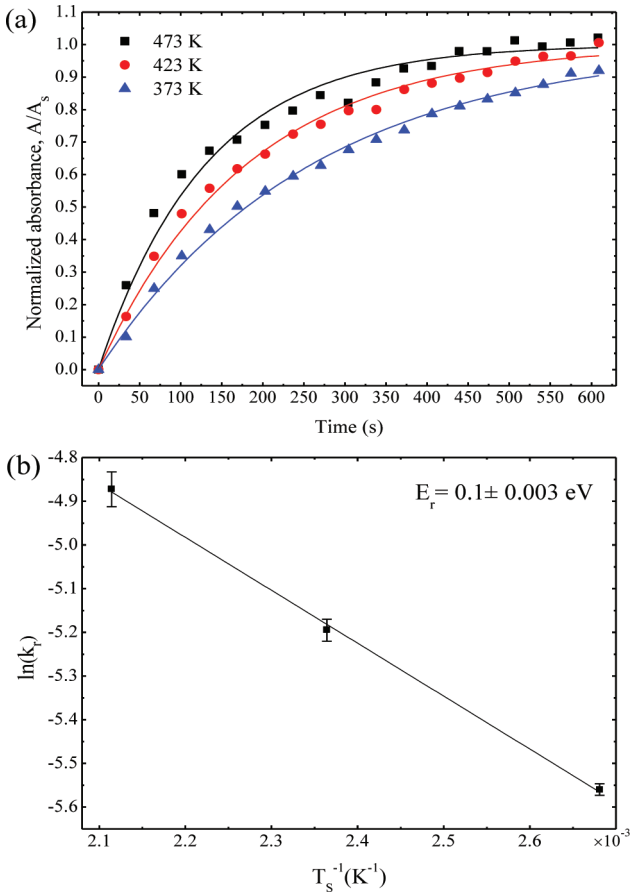

Figure 8. (a) Normalized absorbance as a function of UV irradiation time of the photoinduced species in the 1205−1409 cm^{-1} region during the first 10 min UV irradiation period at T_s being 373, 423, and 473 K. The solid curves show the best fits to the experimental data using first-order reaction kinetics. (b) Arrhenius plot of the formation rate constant, $\ln(k_r)$ vs T_s^{-1}.

natural to attribute the increasing concentration of coordinated $SO_x^{\delta-}$ surface species as a function of T_s to an increasing O vacancy concentration.[1,21,22] An Arrhenius analysis yields an apparent activation energy of E_r= 0.1 eV (Figure 8b). This is, however, much lower than reported O vacancy formation energies in TiO_2 bulk deduced from diffusion measurements (2.1−2.8 eV)[26−28] and also smaller than values obtained from surface diffusion studies in nanocrystalline TiO_2 films (1−1.5 eV).[28] We note, however, that band gap irradiation has been reported to enhance O diffusion in nanocrystalline anatase TiO_2.[29] Alternatively, surface O vacancies may form due to OH condensation reactions.[1,3] The latter is relevant since the surface becomes dehydroxylated and HSO_3^- species are oxidized at elevated temperatures as shown by the FTIR data.

3.3. Modification and Stability of Surface Acid Properties by SO_2 Photofixation. Figure 9 shows the IR

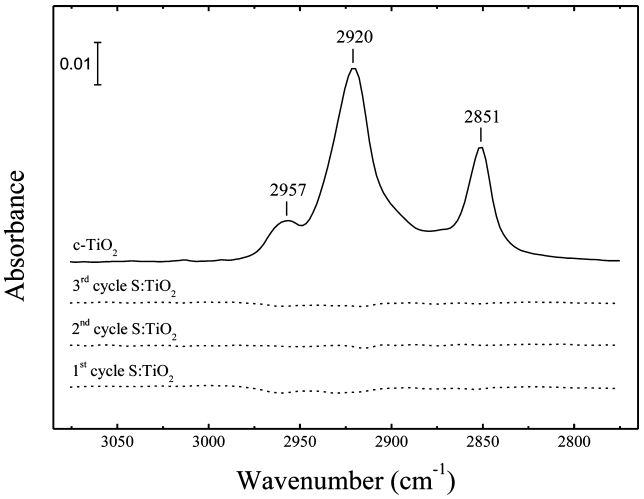

Figure 9. Infrared absorbance spectra for pure and SO_2-modified TiO_2 crystalline films (denoted S/TiO_2) prepared at T_s = 473 K recorded after each of 3 cycles of spin coating of stearic acid on the same S/TiO_2 film with intermittent rinsing between each measurement, showing that the surface acid properties remain after repeated usage of the SO_2-modified TiO_2 film.

absorbance, which is proportional to the concentration, of stearic acid on c-TiO_2 film and on c-TiO_2 films treated in 50 ppm SO_2 under UV irradiation at T_s = 473 K after three repeated spin coating and cleaning cycles. The latter measurements were performed after subsequent stearic acid spin coatings, as described above. As we have previously shown, it is evident that the concentration of stearic acid is negligible on the SO_2 photofixated c-TiO_2 films.[11] We note that there is a fundamental difference between measurements performed for assessment of photofixation of SO_2 and for the adherence of stearic acid onto TiO_2 films. The former is performed as an in situ test, and the later is performed in open air where the film is exposed to air. The S/TiO_2 films in the latter case become hydroxylated upon exposure to humid air. However, in this process, the surface sites that already have been occupied by SO_2 by reactions with O vacancies are not hydroxylated (reactions 4 and 6). This means that basic OH groups that are consumed during UV illumination cannot be replenished (reactions 3 and 5). This implies that SO_2 photofixation modifies the surface acidity in two ways: both by addition of acidic SO_x species and by irreversible removal of basic OH groups. The former can be attributed to the acidic properties of the sulfite and sulfate species, which chemically act as Brønstedt acid sites.[14] The latter is associated with basic OH groups which act as coordinating sites for stearic acid to be adsorbed to the surface

dx.doi.org/10.1021/am201253y | ACS Appl. Mater. Interfaces 2012, 4, 672−679

via the esterification process. The results in Figure 9 show that the oleophobic properties remain after repeated spin coating and rinsing of the films. These results indicate that the UV-induced low-temperature SO_2 photofixation process provides a viable method for purposefully modifying the surface acidity of anatase TiO_2, which e.g., can find applications in antigrease or oleophobic surface treatments.

4. CONCLUSIONS

UV irradiation of anatase TiO_2 films in gas containing SO_2 and O_2 at elevated temperatures results in the formation of strongly bonded sulfur species. By combining XPS and in situ FTIR data, the molecular identity of these sulfur species has been identified and a reaction mechanism proposed. It is shown that adsorbed SO_2 is photo-oxidized to sulfide and sulfate surface species, where the latter are thermodynamically more stable. The results suggest a mechanism where band gap irradiation of TiO_2 yield reactive oxygen species which oxidize SO_2. At temperatures between 373 and 523 K, significant amounts of O vacancies form and provide reaction sites that promote the formation of strongly bonded, coordinated sulfate species. These species desorb at temperatures above 523 K. The surface becomes acidic upon SO_2 photofixation at elevated temperatures, which is manifested in weak adherence of stearic acid. Repeated spin coating and rinsing shows that the surface acidity is persistent on the SO_2 photofixated films and suggests means to fabricated oleophobic and antigrease coatings.

AUTHOR INFORMATION

Corresponding Author

*Phone: +46 (0) 18 4713132. Fax: +46 (0) 18 4713270. E-mail: Zareh.Topalian@angstrom.uu.se.

ACKNOWLEDGMENTS

The authors thank Dr. Esteban Avendaño Soto for his support with XPS data analysis and Andreas Mattsson for FTIR measurements.

REFERENCES

(1) Diebold, U. *Surf. Sci. Rep.* **2003**, *48*, 53.
(2) Fujishima, A.; Zhang, X.; Tryk, D. A. *Surf. Sci. Rep.* **2008**, *63*, 515.
(3) Henrich, V. A.; Cox, P. A. *The Surface Science of Metal Oxides*; Cambridge University Press: Cambridge, U.K., 1994.
(4) Armor, J. N. *Appl. Catal., B* **1992**, *1*, 221.
(5) Yanxin, C.; Yi, J.; Wenzhao, L.; Rongchao, J.; Shaozhen, T.; Wenbin, H. *Catal. Today* **1999**, *50*, 39.
(6) Yamazoe, N.; Sakai, G.; Shimanoe, K. *Catal. Surv. Asia* **2003**, *7*, 63.
(7) Topalian, Z.; Smulko, J. M.; Niklasson, G. A.; Granqvist, C. G. *J. Phys.: Conf. Series* **2007**, *76*, 012056.
(8) Yang, T. Y.; Lin, H. M.; Wei, B. Y.; Wu, C. Y.; Lin, C. K. *Rev. Adv. Mater. Sci.* **2003**, *4*, 48.
(9) Occupational Safety and Health Administration (OSHA); http://www.osha.gov, Access date: 14 Feb. 2011.
(10) Fox, M. A.; Dulay, M. T. *Chem. Rev.* **1993**, *93*, 341.
(11) Topalian, Z.; Niklasson, G. A.; Granqvist, C. G.; Österlund, L. *Thin Solid Films* **2009**, *518*, 1341.
(12) Mattsson, A.; Leideborg, M.; Larsson, K.; Westin, G.; Österlund, L. *J. Phys. Chem. B* **2006**, *110*, 1210.
(13) Moulder, J. F.; Stickle, W. F.; Sobol, P. E.; Bomben, K. D. *Handbook of X-Ray Photoelectron Spectroscopy*; Physical Electronics: Eden Prairie, MN, 1995.
(14) Davydov, A. A. *Molecular Spectroscopy of Oxide Catalyst Surfaces*; John Wiley & Sons: Chichester, 2003.
(15) Forney, D.; Kellogg, C. B.; Thompson, W. E.; Jacox, M. E. *J. Chem. Phys.* **2000**, *113*, 86.
(16) Luo, T.; Vohs, J. M.; Gorte, R. J. *J. Catal.* **2002**, *210*, 397.
(17) Shor, A. M.; Dubkov, A. A.; Rubaylo, A. I.; Pavlenko, N. I.; Sharonova, O. M.; Anshits, A. G. *J. Mol. Struct.* **1992**, *267*, 335.
(18) Beck, D. D.; White, J. M.; Ratcliffe, C. T. *J. Phys. Chem.* **1986**, *90*, 3123.
(19) Nakamoto, K. *Infrared and Raman Spectra of Inorganic and Coordination Compounds; Part II*; John Wiley & Sons: New York, 1997.
(20) Mshchenko, A. I. *Kinet. Katal.* **1967**, *8*, 704.
(21) Lu, G.; Linsebigler, A.; Yates, J. T. Jr. *J. Phys. Chem.* **1994**, *98*, 11733.
(22) Wendt, S.; Sprunger, P. T.; Lira, E.; Madsen, G. K. H.; Li, Z.; Hansen, J. O.; Matthiesen, J.; Blekinge-Rasmussen, A.; Laegsgaard, E.; Hammer, B.; Besenbacher, F. *Science* **2008**, *320*, 1755.
(23) Primet, M.; Pichat, P.; Mathieu, M.-V. *J. Phys. Chem.* **1971**, *75*, 1216.
(24) Primet, M.; Pichat, P.; Mathieu, M.-V. *J. Phys. Chem.* **1971**, *75*, 1221.
(25) Dohnálek, Z.; Lyubinetsky, I.; Rousseau, R. *Prog. Surf. Sci.* **2010**, *85*, 161.
(26) Arita, M.; Hosoya, M.; Kobayashi, M.; Someno, M. *J. Am. Ceram. Soc.* **1979**, *62*, 443.
(27) Derry, D. J.; Lees, D. G. *J. Phys. Chem. Solids* **1981**, *42*, 57.
(28) Höfler, H. J.; Hahn, H.; Averback, R. S. *Defect Diffus. Forum* **1991**, *75*, 195.
(29) Mattsson, A.; Leideborg, M.; Persson, L.; Westin, G.; Österlund, L. *J. Phys. Chem. C* **2009**, *113*, 3810.